AIP | Applied Physics Letters

Quantum dot Ge/TiO2 heterojunction photoconductor fabrication and performance

Carena P. Church, Elayaraja Muthuswamy, Guangmei Zhai, Susan M. Kauzlarich, and Sue A. Carter

Citation: Appl. Phys. Lett. **103**, 223506 (2013); doi: 10.1063/1.4826916
View online: http://dx.doi.org/10.1063/1.4826916
View Table of Contents: http://apl.aip.org/resource/1/APPLAB/v103/i22
Published by the AIP Publishing LLC.

Quantum dot Ge/TiO_2 heterojunction photoconductor fabrication and performance

Carena P. Church,[1] Elayaraja Muthuswamy,[2] Guangmei Zhai,[3] Susan M. Kauzlarich,[2] and Sue A. Carter[1,a)]
[1]*Department of Physics, University of California Santa Cruz, Santa Cruz, California 95064, USA*
[2]*Department of Chemistry, University of California Davis, Davis, California 95616, USA*
[3]*Key Laboratory of Interface Science and Engineering in Advanced Materials of Ministry of Education, Taiyuan University of Science and Technology, Taiyuan, Shanxi 030024, People's Republic of China*

(Received 20 May 2013; accepted 22 September 2013; published online 25 November 2013)

Spun cast TiO_2-Ge quantum dot (QD) heterojunction type photodetectors have been fabricated and characterized, with interest paid to photocurrent enhancements related to device design. Performance as a function of absorber layer thickness, QD size, and back contact is investigated. We have achieved ultra-thin ($\sim$200 nm) devices with photocurrents at 0.5 V of 10^{-4} A cm^{-2} while the thickest devices have photocurrents at 0.5 V of 10^{-2} A cm^{-2} with on-off ratios $>$100, which represents 5 orders of magnitude increase in photocurrents over previously fabricated Ge QD devices. At 0.5 V bias, the currents in our devices are competitive with thin-film Ge photovoltaics.
 [http://dx.doi.org/10.1063/1.4826916]

Group IV semiconductors have long been used in photodetectors, photovoltaics (PV), sensors, and light-emitting diodes,[1,2] but recently, group IV colloidal quantum dots (CQD) have garnered increased interest in the optoelectronics field due to their lower toxicity compared to lead- and cadmium-containing colloidal QD systems, low-cost solution processability, desirable ability to tune electrical properties, increased response in the IR region, and potential for higher conversion efficiencies in PV devices due to Multiple Exciton Generation (MEG).[3–8] Specifically, Germanium (Ge) QDs have drawn interest due to their narrow bulk bandgap, which can be readily tuned by quantization to the optimal energies for both maximum power conversion efficiencies (η) and MEG enhancements to η,[9] and their large exciton Bohr radius which should provide the necessary quantum confinement effects.[10,11] So far, however, unary group IV QD systems have not been widely studied, mainly due to difficult colloidal syntheses compared to the easier binary IV CQD syntheses. Recently, unary IV solution syntheses have begun to catch up with II-VI and IV-VI syntheses, enabling groups to begin studying Ge CQD optoelectronic properties. Holman *et al.* have focused on Ge QD field-effect transistors fabricated via drop casting onto Si wafers, while Xue *et al.* focus on hybrid Ge nanoparticle (NP)-polymer blend photodetectors fabricated via drop casting Ge NP-P3HT ink blend.[12,13] Although the hybrid photodetectors show good responsivity with photocurrents on the order of 10^{-9} A cm^{-2}, it is unclear what role the polymer is playing. To improve and isolate Ge performance, we turn to fabricating heterojunction type devices, which have been studied in depth for II-VI and IV-VI CQD systems and are so far the only QD device type to show the MEG effect.[7,8]

Here, we report on the fabrication and characterization of photoconductive spun-cast heterojunction devices with a window layer of TiO_2 and Ge QDs as the active layer. Our treated films are not insulating and require no anneal, potentially lowering future production costs. We focus on performance improvements achieved through variations in absorber layer thickness, QD size, and back contact. Our best devices show improvement in photocurrents by 5 orders of magnitude over previous Ge QD devices[13] and have photocurrents at 0.5 V comparable to Ge thin-film photovoltaics.[14] This work demonstrates that Ge QD heterojunction devices are a promising system for future photoelectric devices with ample room for improvement and optimization, while these devices represent a pathway to cheaper, more accessible photovoltaics.

A transmission electron microscope (TEM) image of the 4.3 ± 1.0 nm Ge QDs used (TEM images of the 6.3 ± 1.0 nm and 8.9 ± 1.7 nm can be found in the supplementary material[15]), a cross-sectional high-resolution scanning electron microscope (HR-SEM) image of the device stack, along with a cartoon of the device structure and energy band diagrams of our devices are shown in Fig. 1. The colloidal Ge QDs were synthesized at UC Davis using a microwave-assisted heating route prescribed via literature.[16] TiO_2 sol-gel was prepared by the standard procedure described previously.[17] Both TiO_2 sol-gel and NP pastes were spin-coated onto a cleaned glass substrate with pre-patterned Indium Tin Oxide (ITO) electrodes of 150 nm thickness sequentially. Each TiO_2 layer was sintered at 450 °C for 30 min in air after deposition to improve conductivity. The Ge QD film was then deposited onto the TiO_2 film by spin-coating the QD ink in a nitrogen-filled glove box followed by immersing the substrate into a solution of 1 M hydrazine, pyridine, or 1,2-ethanedithiol (EDT) in acetonitrile for 15 s to facilitate film formation and increase electronic coupling between the QDs. The thickness of the QD film is controlled by spin speed, number of cycles, and concentration of the QD ink. Finally, 100 nm of silver, gold, or aluminum contact was thermally evaporated under high vacuum; the area of each device formed is 0.03 cm^2.

Current density-voltage (J-V) curves were taken in the dark and under calibrated AM1.5G illumination. The

a)Electronic mail: sacarter@ucsc.edu

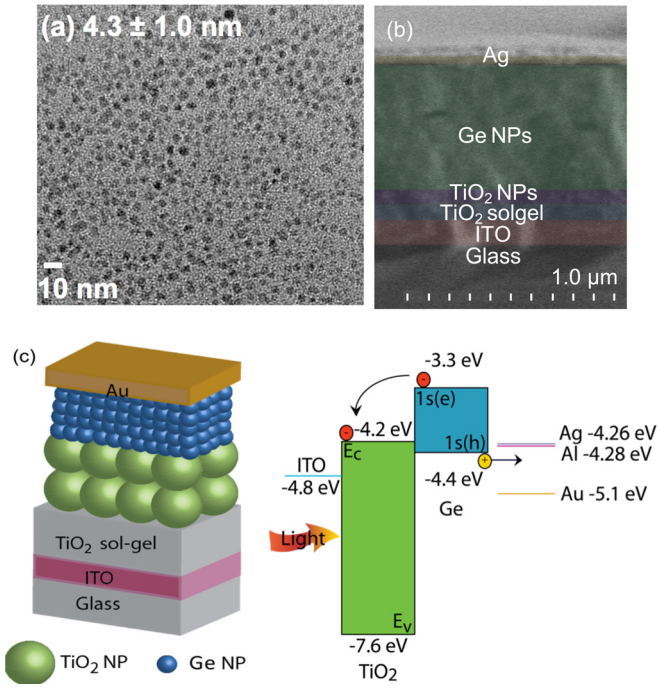

FIG. 1. (a) TEM image of the 4.3 ± 1.0 nm Ge QDs used to fabricate devices. (b) HRSEM cross-sectional image of device stack. (c) Cartoon of device structure with energy band diagrams of the TiO_2-Ge heterojunction type devices studied in this paper.

topography and thickness of Ge QD films were measured by both HRSEM and an atomic force microscope (AFM). All device characterizations, unless otherwise stated, were carried out in a nitrogen-filled glove box at an oxygen concentration below 50 ppm.

As received, the oleylamine capped NPs are incapable of forming films via multi-layer spin- or dip-coating. Unlike previously studied group IV-VI QD systems, our Ge QDs are also incapable of forming films when exchanged with 1,2-ethanedithiol,[7] and we found that films fabricated with these oleylamine-capped QDs remain soluble until ligand exchange with a suitable amine is carried out. AFM measurements give a surface RMS roughness of 12 nm for the Ge QD film, indicating a rough, mesoporous layer.

Room-temperature absorbance of the colloidal Ge QDs capped with oleylamine in hexane and the absorbance of films formed by hydrazine exchange on a quartz substrate (supplementary material, Fig. S2) shows both the pre and post-hydrazine treated spectra appear identical and have no observable exciton peak, consistent with previous literature reports.[18–20] FTIR spectra (supplementary material, Fig. S3) show that hydrazine treatments result in the suppression of both symmetric and anti-symmetric stretching peaks associated with C-H bonds from oleylamine, indicating replacement of oleylamine on the surface of the QD with hydrazine, in contrast to recent reports with alloyed Ge NPs.[21] Of EDT, pyridine, and hydrazine, we find that only exchange with hydrazine is suitable for film formation (supplementary material, Fig. S5(a)). Tauc plots obtained for both liquids and films (supplementary material, Fig. S5(b)), with film fits from a linear regression giving bandgaps ranging from 0.87 eV to 1.15 eV, which are comparable to the values reported by Neale *et al.*[18] for a similar size range.

Initial devices were marred by poor QD film quality. Previous results[22] from similarly structured PbS-TiO_2 devices indicate a rough, mesoporous QD layer could decrease charge transport, which we observed in our early, thin devices. We note that considering the roughness of TiO_2 nanoparticle film (supplementary material, Fig. S6) and penetration of QDs into the TiO_2 NP film, the actual thickness of Ge QD films may be up to 100 nm less than the measured Ge QD layer thickness. This mesoporous interface between TiO_2 and Ge in our devices should allow for sufficient absorption while also aiding exciton dissociation.[7]

As a first step in understanding our devices, we look at thickness versus performance. All devices in the thickness-dependence study employ the largest QDs with diameter of 8.9 ± 1.7 nm. Fig. 2(a) shows the J-V curves for devices as a function of increasing active layer thickness, with thickness denoted by the number of spin + hydrazine treatment cycles, N. As a function of thickness, the photocurrents initially decrease, then increase through 1000 nm (N = 10), before dropping off again (N > 10) due to the trade-off between charge extraction (thinner devices) and increased

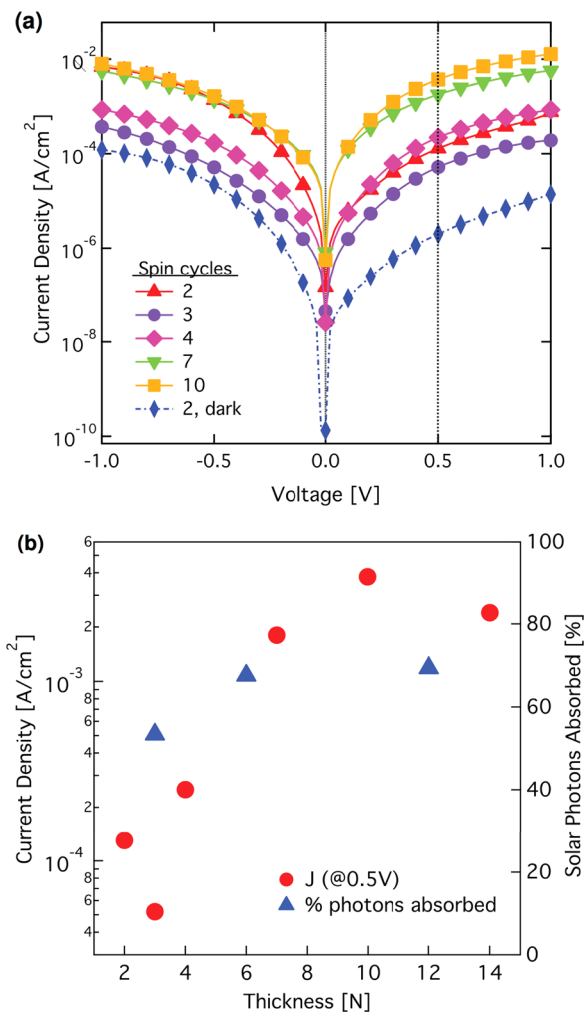

FIG. 2. (a) J-V curves for the largest QDs vs. absorber layer thickness. Thicknesses are indicated by N, where N is the number of layers applied sequentially via spin-coating followed by a brief soak in hydrazine. N = 1 is roughly equivalent to 100 nm. (b) Average photocurrents in our devices at a 0.5 V bias and percentage of solar photons absorbed, as a function of device thickness.

photocurrents due to increased absorption (thicker devices). We attribute smaller photocurrents found in thinner layers to incomplete absorption of photons and shunting due to poor film quality.

Our early device performance was predominantly limited by this shunting. For our thinnest devices, film improvements lead to shunting decreases and performance becomes recombination-limited. For thicker films, film quality remains an issue. The thicker films remain visibly rougher, possibly introducing a larger number of interfacial recombination sites. Fig. 2(b) shows the average photocurrents in our devices at a 0.5 V bias and percentage of solar photons absorbed, both as a function of device thickness. Based on absorption from 400–1000 nm, we find our photocurrents are limited mostly by recombination, since films with $N > 10$ (thickness >1 μm) absorb almost 80% of all available photons without considering IR absorption. At 0.5 V, the best photocurrents are 13 mA cm^{-2} with on-off ratios of greater than 100.

Assuming ideal diode characteristics and 100% absorption, the photocurrent is simply a function of bandgap.[23] For bandgaps ranging from 0.87 eV to 1.15 eV, the maximum possible photocurrent ranges from $\sim$40 mA cm^{-2} to $\sim$56 mA cm^{-2}. 80% absorption over the whole spectrum brings the lower limit down to 32 mA cm^{-2}, which is only a few mA higher than our best devices.

To better understand the response mechanism behind our Ge NPs and confirm improvements over the previously reported hybrid Ge QD photoelectric devices, we tried Schottky-type devices with Ge NPs and various back contacts. All of these devices were resistive, likely due to leakiness across the Ge NP layer. The TiO_2 sol-gel layer prevents this leakiness in our heterojunction devices, while the TiO_2 NP layer aids in charge extraction. Additionally, we isolate improvement by looking at the absorption of individual components along with external quantum efficiency (EQE) of the device. Fig. S6 shows UV-Vis absorption spectra of the ITO layer on glass, Ge NPs only, TiO_2 layer, and full TiO_2-Ge NP heterojunction devices (supplementary material, Fig. S7); however, signals were too low for reliable EQE measurements. The large increase in absorption from TiO_2 only to full device stack indicates the window layer alone is not responsible for the increases in photocurrents.

To examine the effect of QD size on device performance, we held the thickness of Ge layers in subsequent devices constant at $\sim$300 nm. In Fig. 2, J-V curves for devices made with each size QD are shown. These trends hold over many devices and indicate the largest QDs yield best performance, with best photocurrents at 0.5 V around 22 mA cm^{-2} while both smaller sizes have currents at 0.5 V of 10^{-3} A cm^{-2}. This is expected, as currents increase with QD size due to a larger percentage of the solar spectrum being available for carrier generation. Previous size-dependent studies with binary group IV-VI QD systems have shown evidence for increased mobilities with increasing QD size due to the smaller number of hops a carrier must take between generation sites and extraction interfaces,[24] which our results seem to support. Additionally, optical characterizations of the Ge QDs used suggest the smaller NPs become increasingly amorphous,[16] which could also play a role in their lower performance.

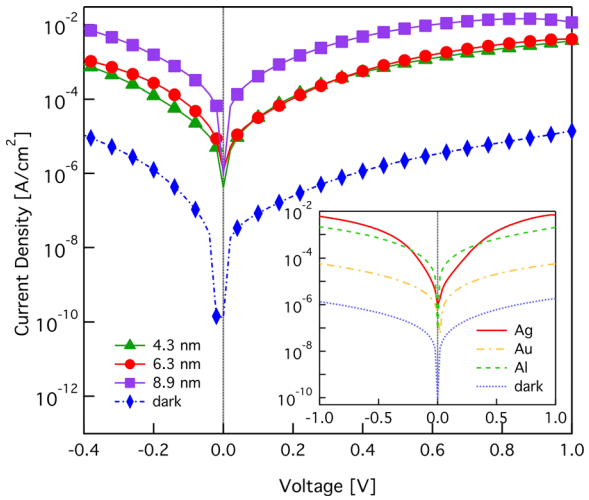

FIG. 3. J-V characteristics of devices made with different sized QDs. All devices shown have absorber layer thickness $\sim$300 nm. Inset: J-V curves show the difference in performance when back contact is varied.

Another device design choice involves proper selection of the back contact to facilitate non-impeded charge extraction. Fig. 3 shows J-V characteristics of devices made with gold, silver, and aluminum back contacts. Ag and Al should both form ohmic contacts; however, we find that Ag is the best performer in terms of favoring hole extraction. As seen in the inset of Fig. 3, the choice of contact can increase performance by up to 3 orders of magnitude, with Ag backed devices having currents 5 orders of magnitude greater than previous hybrid Ge/polymer devices.[13]

Although we have achieved large increases in photocurrents, our devices behave as photodetectors, not photovoltaics, in that they do not have any meaningful open-circuit voltage. Based on our approximated energy levels, we should observe photovoltages <0.3 V. Our low photovoltages are likely a result of poor charge extraction at the electrode.

Additionally, it is unclear whether hydrazine is on the surface of the QD, as the expected Ge-N peak at 650 cm^{-1} in the FTIR spectra (supplementary material, Fig. S2) is missing.[25] Our EDT + hydrazine devices perform more poorly than the majority of hydrazine-only devices (supplemental material, Fig. S8). The hydrazine treatment was applied first in our trials, as an initial EDT treatment renders the film soluble. Other experiments have shown that hydrazine not only replaces the capping ligand but also acts on the transport mechanisms and in some cases renders the QDs n-type,[26,27] which could be the cause of similar results between hydrazine + EDT and hydrazine only films. Recent theoretical studies indicate H-bonded ligands create sub-valance band donor states, further limiting the available photovoltage.[28]

In conclusion, we have fabricated and studied TiO_2-Ge NP photodetectors, with particular interest paid to performance enhancements related to device design, Ge layer thickness, and NP size. We have achieved ultra-thin ($\sim$200 nm) devices with photocurrents at 0.5 V of 10^{-4} A cm^{-2} while the thickest devices have photocurrents at 0.5 V of 10^{-2} A cm^{-2} with on-off ratios >100, which represents 5 orders of magnitude increase in performance over previously fabricated Ge CQD devices. The best devices have photocurrents of

23 mA cm^{-2} at 0.5 V bias, which is half of the ideal maximum 46 mA cm^{-2} and comparable to those achieved in thin-film bulk Ge photovoltaic devices,[14] opening the door for the use of Ge QDs in energy conversion applications. We note that the junction used herein is not optimal and upon further improvement or change in device structure, both increased photocurrents and photovoltages should be expected. Various device structures are being designed with the dual goals of achieving similarly high photocurrents at 0 V bias and increasing photovoltages.

This research was supported NSF SOLAR Program DMR-1035468. SAC also acknowledges support from the Advanced Studies Laboratory at NASA Ames.

[1]S. Healy and M. Green, Sol. Energy Mater. Sol. Cells **28**, 273 (1992).
[2]J. Michel, J. Liu, and L. C. Kimerling, Nat. Photonics **4**, 527 (2010).
[3]R. D. Schaller and V. I. Klimov, Phys. Rev. Lett. **92**, 186601 (2004).
[4]A. J. Nozik, M. C. Beard, J. M. Luther, M. Law, R. J. Ellingson, and J. C. Johnson, Chem. Rev. **110**, 6873 (2010).
[5]J. Tang and E. H. Sargent, Adv. Mater. **23**, 12 (2011).
[6]H. W. Hillhouse and M. C. Beard, Curr. Opin. Colloid Interface Sci. **14**, 245 (2009).
[7]G. Zhai, C. P. Church, A. J. Breeze, D. Zhang, G. B. Alers, and S. A. Carterm, Nanotechnology **23**, 405401 (2012).
[8]O. E. Semonin, J. M. Luther, S. Choi, H.-Y. Chen, J. Gao, A. J. Nozik, and M. C. Beard, Science **334**, 1530 (2011).
[9]M. C. Hanna and A. J. Nozik, J. Appl. Phys. **100**, 074510 (2006).
[10]J. Shieh, H. Chen, T. Ko, H. Cheng, and T. Chu, Adv. Mater. **16**, 1121 (2004).
[11]C. Bostedt, T. van Buuren, T. M. Willey, N. Franco, L. J. Terminello, C. Heske, and T. Moller, Appl. Phys. Lett. **84**, 4056 (2004).
[12]Z. C. Holman, C.-Y. Liu, and U. R. Kortshagen, Nano Lett. **10**, 2661 (2010).
[13]D.-J. Xue, J.-J. Wang, Y.-Q. Wang, S. Xin, Y.-G. Guo, and L.-J. Wan, Adv. Mater. **23**, 3704 (2011).
[14]J. van der Heide, N. E. Posthuma, G. Flamand, and J. Poortmans, AIP Conf. Proc. **890**, 129 (2007).
[15]See supplementary material at http://dx.doi.org/10.1063/1.4826916 for more experimental information, additional TEM and AFM images, FTIR and UV-Vis absorbance spectra, Tauc plots, and additional JV curves.
[16]E. Muthuswamy, A. S. Iskandar, M. M. Amador, and S. M. Kauzlarich, Chem. Mater. **25**, 1416 (2013).
[17]A. C. Arango, L. R. Johnson, V. N. Bliznyuk, Z. Schlesinger, S. A. Carter, and H.-H. Hörhold, Adv. Mater. **12**, 1689 (2000).
[18]D. A. Ruddy, J. C. Johnson, E. R. Smith, and N. R. Neale, ACS Nano **4**, 7459 (2010).
[19]Z. C. Holman and U. R. Kortshagen, Nano Lett. **11**, 2133 (2011).
[20]Z. C. Holman and U. R. Kortshagen, Appl. Phys. Lett. **100**, 133108 (2012).
[21]D. A. Ruddy, P. T. Erslev, S. E. Habas, J. A. Seabold, and N. R. Neale, J. Phys. Chem. Lett. **4**, 416 (2013).
[22]T. Ju, R. L. Graham, G. Zhai, Y. W. Rodriguez, A. J. Breeze, L. Yang, G. B. Alers, and S. A. Carter, Appl. Phys. Lett. **97**, 043106 (2010).
[23]S. M. Sze and K. K. Ng, *Physics of Semiconductor Devices*, 3rd ed. (Wiley-VCH Verlag, Hoboken, 2006).
[24]Y. Liu, M. Gibbs, J. Puthussery, S. Gaik, R. Ihly, H. W. Hillhouse, and M. Law, Nano Lett. **10**, 1960 (2010).
[25]F. Berg Rasmussen, R. Jones, and S. Öberg, Phys. Rev. B **50**, 4378 (1994).
[26]D. V. Talapin and C. B. Murray, Science **310**, 86 (2005).
[27]J. M. Luther, M. C. Beard, Q. Song, M. Law, R. J. Ellingson, and A. J. Nozik, Nano Lett. **7**, 1779 (2007).
[28]C. G. V. de Walle and J. Neugebauer, Nature **423**, 626 (2003).